Available online at www.sciencedirect.com
SCIENCE DIRECT
Carbohydrate Research 341 (2006) 598–609
Carbohydrate RESEARCH

Differentiation of the fucoidan sulfated L-fucose isomers constituents by CE-ESIMS and molecular modeling

Bérangère Tissot,[a,†] Jean-Yves Salpin,[a] Michael Martinez,[b] Marie-Pierre Gaigeot[a,b] and Régis Daniel[a,*]

[a]*Laboratoire Analyse et Environnement, UMR 8587 CNRS, Université d'Evry Val d'Essonne, F-91025 Evry, France*
[b]*Laboratoire Modélisation des Systèmes Moléculaires Complexes, Université d'Evry Val d'Essonne, F-91025 Evry, France*

Received 2 September 2005; received in revised form 23 November 2005; accepted 23 November 2005
Available online 17 January 2006

Abstract—α-L-Fucose, the monosaccharide component of fucoidan, is found in the polysaccharide mainly as its sulfated form where sulfate groups are in position 2 and/or 4 and/or 3. The correlation between biological activities and structure of fucoidan requires the determination of the sulfation pattern of the fucose residues. Therefore, it is of importance to discriminate between the isobaric sulfated fucose isomers. For this purpose, the three isomers 2-*O*-, 3-*O*-, and 4-*O*-sulfated fucose have been analyzed using electrospray ion trap mass spectrometry and capillary electrophoresis. The results reported herein show that it is possible to differentiate between these three positional isomers of sulfated fucose based on their fragmentation pattern upon MS/MS experiments. 3-*O*-Sulfated fucose was characterized by the loss of the hydrogenosulfate anion HSO_4^- as the main fragmentation product, while the two other isomers 2-*O*-, and 4-*O*-sulfated fucose exhibited cross-ring fragmentation yielding to distinctive $^{0,2}X$ and $^{0,2}A$ daughter ion, respectively. A computational study of the conformation of the sulfated fucose isomers was carried out providing an understanding of the fragmentation pattern with respect to the position of the sulfate group.

Keywords: Sulfated fucose; Fucoidan; ESIMS; Capillary electrophoresis; Molecular modeling; Isomeric structures differentiation

1. Introduction

Structural analysis of carbohydrates present in living systems is recognized as one of the most challenging task of glycosciences, given the structural complexity related to the monosaccharide composition, the various isomeric forms, the degree of branching and polymerization, and the difficulty in detection.[1,2] The huge structural diversity of carbohydrates has given rise to the concept of isomer barrier that represents a major hindrance in the structure–activity relationship establishment.[3] Among all the biopolymers, carbohydrates offer the largest potential of information owing their incomparable variety of combinations and of regioselective modifications of their constitutive monosaccharides.[4] Sulfation is one of the major modifications, as many biological activities of carbohydrates are driven by charge pattern recognition upon interaction with targeted proteins.[5] Electrospray ionization mass spectrometry is widely recognized as a powerful and highly sensitive analytical method for the characterization of sulfated oligosaccharides that ionize readily in negative ESIMS mode.[6–8] Furthermore ESIMS allows on-line coupling to liquid-phase separation techniques, which is useful to solve complex mixture prior to MS analysis.[9–12]

The differentiation of saccharide isomers by mass spectrometry could be achieved using collisional-induced dissociation (CID).[8,13–15] The present work addresses

* Corresponding author. Tel.: +33 1 69 47 7641; fax: +33 1 69 47 7655; e-mail: regis.daniel@univ-evry.fr
† Present address: Division of Molecular Biosciences, Imperial College, South Kensington Campus, Exhibition Road, SW7 2AZ London, UK.

0008-6215/$ - see front matter © 2005 Elsevier Ltd. All rights reserved.
doi:10.1016/j.carres.2005.11.029

the discrimination of positional isomers of monosulfated L-fucose by tandem ESIMS using an ion trap and by the on-line coupling of capillary electrophoresis. α-Linked sulfated L-fucose is found as the constitutive unit of fucoidan,[16] a polysaccharide endowed with important activities affecting key biological systems,[17] especially in the inhibition of the coagulation cascade[18] and of the complement system.[19] These biological properties are of great interest because of their potential therapeutic applications,[20–23] but the structural heterogeneity of fucoidan is still a main impediment in the identification of the structural determinants involved in the biological properties.[24–26] It is however established that these properties rely on the sulfate groups, and it is assumed that the recognition of a particular pattern of sulfation may allow specific interaction with targeted proteins. Fucoidan is mainly extracted from the cell wall of marine brown algae and also from some echinoderm organisms. Fucose residues in algae fucoidan have been described as being sulfated at position 2 and/or 4 and/or 3 depending on the algal species (Fig. 1A).[27–31] Although not established, a correlation between algal species and fucoidan structure might exist, which could be useful for structure–activity relationship. Further insights in the structure–activity relationships are expected from the increasing use of the combination of chemical and enzymatic depolymerization of the polysaccharide[32] as it has been previously done for heparin sulfate oligosaccharides.[33–35] In this trend we have previously described enzymatic activities such as fucosidase,[36] fucoidanase[37] and sulfoesterase[38] able to modify algae fucoidan and producing sulfated oligo- and monosaccharides. As ESIMS shows considerable potential for the analysis of these fucoidan-derived sulfated saccharides, it is of importance to determine how the monosulfated fucose isomer constituents of fucoidan can be discriminated using mass

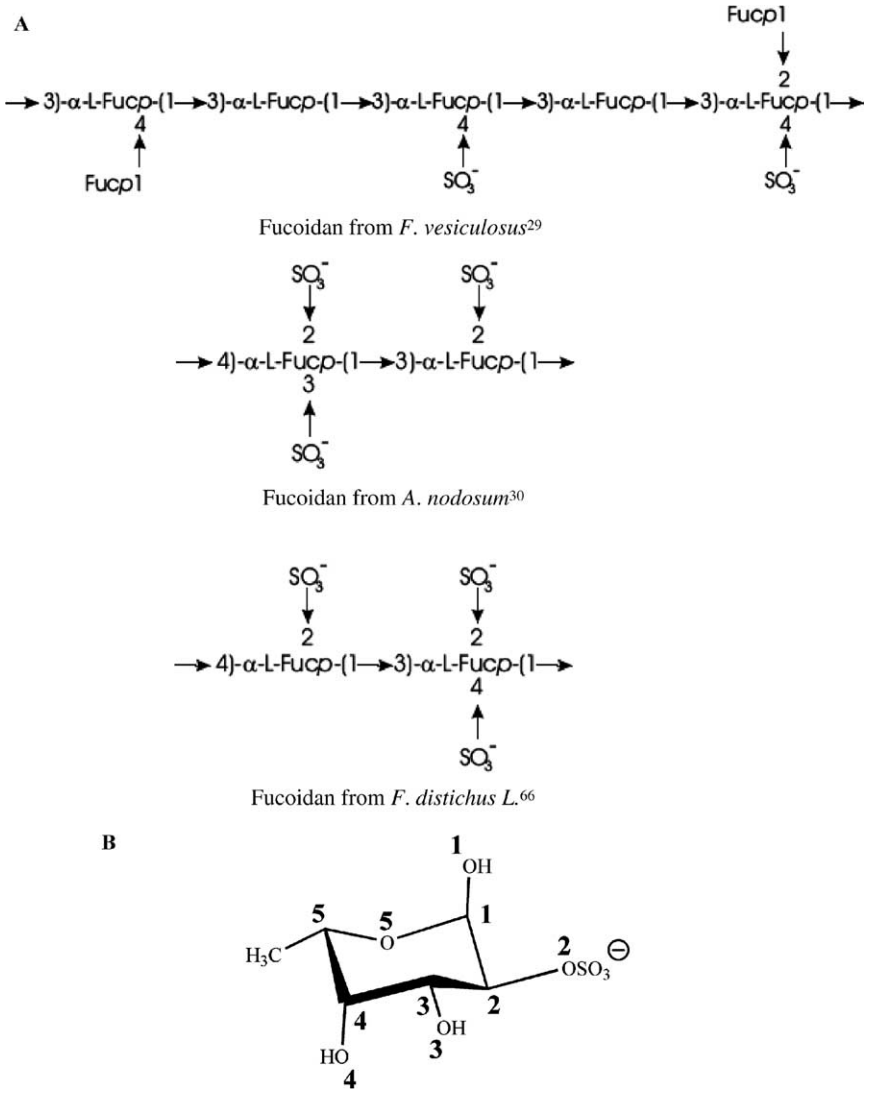

Figure 1. (A) Reported structures of fucoidan extracted from various brown algae. (B) Structure and atomic labeling of the 2-*O*-sulfated fucopyranosyl ring.

spectrometry. To this end, electrospray ionization in the negative mode has been used in conjunction with MS/MS experiments and capillary electrophoresis. To help in the understanding of the fragmentation patterns observed experimentally, computations in the framework of density functional theory have also been carried out.

2. Experimental

2.1. Reagents

The mixtures of the three isomers 2-, 3-, and 4-sulfated L-fucose and of the two isomers 2- and 4-sulfated L-fucose, and the 3-sulfated L-fucose were obtained from Grampian Enzymes (Orkney, Scotland). The mixture of the two isomers 3- and 4-sulfated L-fucose was prepared as previously described.[38] MeOH, ethanol, isopropanol, and acetonitrile were of HPLC Ultra Gradient Grade from Aldrich (Steinheim, Germany). Other chemicals and reagents were obtained from current commercial sources at the highest level of purity available. Water of ultra-pure quality (milliQ system, Millipore, Milford, MA) was used for the preparation of the CE electrolytes and sample solutions.

2.2. Mass spectrometry analysis

ESIMS and ESIMS/MS were carried out on an Esquire 3000+ ion trap mass spectrometer (ITMS) (Bruker Daltonics, Bremen, France). Sulfated monosaccharides were dissolved in MilliQ water at a concentration of 4 μM, and were injected through a syringe pump (74,900 series Cole-Parmer, USA) at 3 μL/min into the electrospray source. All mass spectra were acquired in the negative ionization mode. Data acquisition was performed in the standard resolution mode with a scan speed of 13,000 m/z per second. The nitrogen pressure and flow rate on the nebulizer were 11 psi and 4.0 L/h, respectively, with a drying gas temperature of 300 °C. The capillary voltage was maintained at 4008 V, and the voltage at the capillary exit and at the skimmer were set at −123.8 and −35.9 V, respectively. Other parameters were optimized in order to get the best signal/noise ratio using the smart mode of the mass spectrometer (Esquire Control software, version 5.1). Helium was used as the collision gas in the ion trap at 10^{-5} mbar and a fragmentation amplitude ranging from 0.25 to 0.65 was applied.

2.3. Capillary electrophoresis and CE-ESIMS

Capillary electrophoresis experiments were performed with an Agilent HP^{3D} CE instrument (Agilent Technologies, Waldbronn, Germany) equipped with an on-column diode-array detector, an autosampler and a power supply able to deliver up to 30 kV, and interfaced with a Hewlett–Packard Kayak XA computer. The HP^{3D} CE ChemStation software was used for instrument control and data collection. Bare fused-silica capillaries (50 μm i.d., 360 μm o.d.) internally uncoated were from Phymep (Paris, France). New capillaries were conditioned by successive flushes with 1 M, 0.1 M NaOH and with water for 10, 5, and 10 min, respectively. Capillaries were rinsed with water and air-dried when not in use.

Ammonium acetate buffer (13 mM, pH 9.2) was used as CE background electrolyte (BGE) and was filtered through 0.2 μm filter units before use. BGE contained 0.6 mM 1,3,5-benzenetricarboxylic acid (trimesic acid) used as UV background chromophore allowing detection by indirect UV absorbance at 200 nm. The acquisition rate was 10 points/s. The capillary was thermostatically controlled at 25 °C. CE experiments were performed in normal polarity by applying a 20 kV (electric field 570 V/cm) positive separation voltage over a 35 cm capillary length (26.5 cm to detector). Prior to each sample injection, the capillary was rinsed with the separation electrolyte for 5 min. Samples of sulfated fucose mixtures were diluted at 10^{-5} M in water and loaded hydrodynamically by applying 50 mbar at the capillary inlet for 4 s. Capillary was equilibrated with BGE-trimesic acid flushed for 5 min between each run.

CE-MS experiments were carried out by connecting a CE capillary of 98 cm length (21.5 cm to detector) to the mass spectrometer, using a commercial CE-ESIMS sprayer (G1607A, Agilent Technologies). The same electrolyte and voltage parameters as above were applied for the CE separation. CE separations were performed in normal polarity by applying a 30 kV separation voltage on the inlet electrode, which generated a constant drawing current of 12.5 μA. A 1:1 water–MeOH sheath liquid was delivered at a flow rate of 3 μL/min using an Agilent 1100 LC pump equipped with a 1:100 splitter. Agilent ChemStation software was used for the entire system control, data acquisition, and data analysis. The CE-MS signal, that is, the total ion current (TIC) was acquired starting from the sample injection into the CE capillary. Samples of sulfated fucose mixtures were diluted at 10 mM in water and loaded hydrodynamically by applying 50 mbar at the capillary inlet for 4 s. Capillary was equilibrated with BGE-trimesic acid flushed for 15 min between each run.

2.4. Computational details

The conformations of the sulfated fucose isomers were built from the starting configuration of neutral fucose in a pyranose $^1C_4$ chair conformation obtained from the CERMAV/Glyco3D database for saccharides and polysaccharides (http://www.cermav.cnrs.fr/glyco3d).

The 2-*O*, 3-*O*, and 4-*O*-sulfated fucose were created by replacing the associated O–H group by O–SO_3^- group. While the pyranose $^1C_4$ chair conformation was retained, bond lengths, valence angles, and torsion angles were free to change during the optimization process by DFT calculations. The H-bonds were then created during the geometry optimization process, thus modifying significantly the initial torsional angles.

Molecular orbital DFT calculations were carried out by using BLYP density functional as implemented in the Gaussian-98 set of programs.[39] Geometry of neutral and 2-*O*-, 3-*O*-, and 4-*O*-sulfated fucose for both α and β anomers have been optimized by combining the BLYP DFT functional with the dp-polarized 6-31++G(d,p) basis set, where diffused and polarized functions have been included on all atoms. All electrons were taken into account in the calculations. The BLYP functional combines the non-local correlation function of Lee et al.,[40] with the Becke 88 exchange functional.[41] DFT/BLYP/6-31++G(d,p) calculations were proved to give very good agreements with experiments, on geometries and frequencies for many different organic molecular complexes (nucleic acids,[42–45] amino acids,[46–48] sugars[49]). The BLYP functional, which includes exchange and correlation functions, is also known to be well suited to the study of intra- and inter-molecular hydrogen bonds.[42,45,47,48]

Harmonic vibrational frequencies were calculated on each optimized structure, in order to check that the optimized geometry corresponds to an energy minimum on the potential energy surface (check of the absence of any imaginary frequency), and to estimate the zero-point vibrational energy (ZPVE) corrections. All energies reported throughout the text are corrected by the ZPVE.

Hydrogen bond distribution was analyzed upon the commonly used criteria of existence of O_D–H···O_A H-bonds (where O_D and O_A are, respectively, the donor and acceptor oxygens): O_D–H ⩽ 1.5 Å, H···O_A ⩽ 2.4 Å, and $O_DHO_A > 120°$.

3. Results and discussion

3.1. Negative ESIMS analysis of the monosulfated fucose isomers

Fucose (6-deoxygalactose), one of the most abundant deoxyhexoses in Nature, is often found with a sulfate group at positions 2, 3, or 4 (Fig. 1B). We first analyzed a mixture of the three sulfated fucose isomers previously shown from ^{1}H NMR studies to contain[38] 25% of L-Fuc*p*-2-OSO_3^-, 60% of L-Fuc*p*-3-OSO_3^-, 15% of L-Fuc*p*-4-OSO_3^-. The negative ESIMS spectrum of this mixture showed a single peak at *m*/*z* 243 corresponding to the molecular ion $[M-H]^-$ of monosulfated fucose (insert in Fig. 2). The presence of the sulfate group allows a high sensitivity in the negative mode. Fragmentation of the molecular ion at *m*/*z* 243 was carried out using different amplitude values. Under the lowest amplitude, the first daughter ion that appeared was at *m*/*z* 97 corresponding to the hydrogenosulfate anion HSO_4^-. Three other highly abundant daughter ions were also observed at *m*/*z* 139, 183, and 225 as the amplitude was increased. They correspond to cross-ring cleavages for the first two one, and to the dehydration of the monosulfated fucose for the last one (Fig. 2). This fragmentation pattern was compared to that obtained with mixtures containing only two isomers, either the

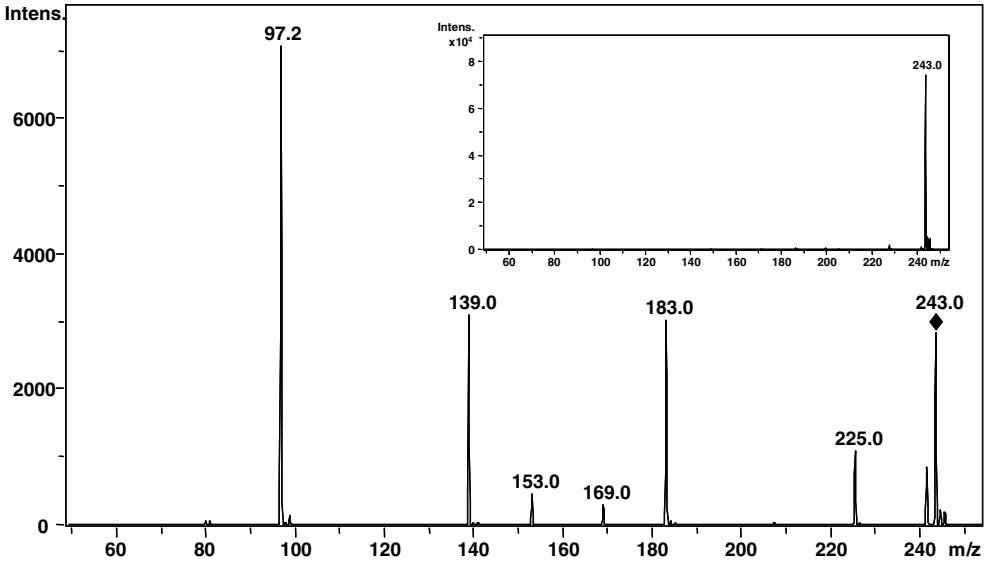

Figure 2. Negative ESIMS/MS spectrum of the mixture of the three 2-*O*-, 3-*O*-, and 4-*O*-sulfated fucose isomers (Full MS spectrum in insert).

4-*O*- and 2-*O*-sulfated fucose (37% and 62%, respectively) or the 4-*O*- and 3-*O*-sulfated fucose (20% and 80%, respectively). The MS/MS spectrum of the mixture containing the 2-*O*- and 4-*O*-sulfated fucose was slightly different from that of the three isomers mixture, since the ions at *m*/*z* 139 and 183 resulting from the opening of the pyranose ring were as abundant as the sulfate anion at *m*/*z* 97 (Fig. 3A). The MS/MS spectrum of the mixture containing the two isomers 3-*O*- and 4-*O*-sulfated fucose exhibited more noticeable differences with regard to the ions relative abundances (Fig. 3B). It is noteworthy that the daughter ion at *m*/*z* 183 was the major fragment while the daughter ions at *m*/*z* 139 and 225 were of a particularly low abundance. These results indicated that the ions issuing from the sulfated fucose fragmentation varied depending on the sulfate position, and suggest that this property may be of great interest for the differentiation of the isomeric monosulfated fucose residues.

The effect of the sulfate position on the fragmentation pattern was confirmed by the negative ESIMS analysis of the 3-*O*-sulfated fucose. This isomer is the only one that has been isolated and purified. The fragmentation of the 3-*O*-sulfated fucose led to only one daughter ion

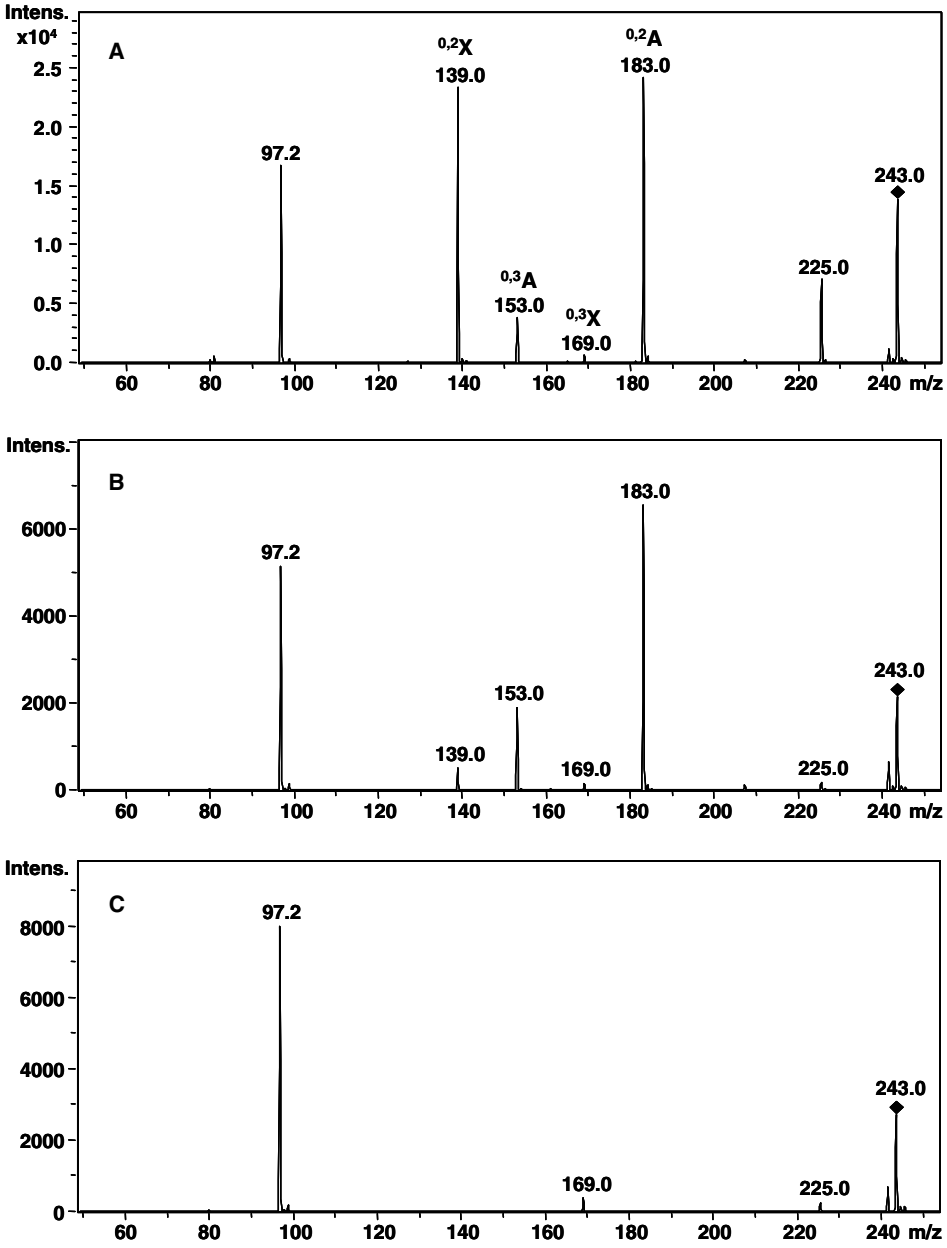

Figure 3. Negative ESIMS/MS spectrum of the mixture of the two isomers 2-*O*- and 4-*O*-sulfated fucose (A), of the two isomers 3-*O*- and 4-*O*-sulfated fucose (B) and of the 3-*O*-sulfated fucose (C).

of high abundance, that is, the sulfate anion at *m*/*z* 97 (Fig. 3C). This contrasts with the fragmentation pattern of the isomer mixtures. No daughter ion corresponding to the opening of the pyranose ring was observed except for a very minor anion at *m*/*z* 169 detected also with the mixtures of isomers. As a consequence, the 3-*O*-sulfated fucose isomer does not contribute to the formation of the daughter ions at *m*/*z* 139 and 183 formed upon the fragmentation of the three isomers mixture. Taking this point into consideration, the MS/MS profile of the two 4-*O*- and 3-*O*-sulfated fucoses mixture reveals that the major daughter ion at *m*/*z* 183 is mainly due to the 4-*O*-sulfated isomer. Besides, the low abundance of the daughter ion at *m*/*z* 139 suggested that the fragmentation of the 4-*O*-sulfated fucose residue yielded predominantly the daughter ion at *m*/*z* 183. Thus the MS/MS profile of the two 4-*O* and 2-*O*-sulfated fucose mixture leads to the conclusion that the daughter ion at *m*/*z* 139 likely mainly results from the 2-*O*-sulfated fucose residue.

3.2. EC-ESI tandem mass spectrometry analysis of the mixture of the sulfated fucose isomers

The determination of the fragmentation pattern of each sulfated fucose isomer present in a mixture could be achieved through their on-line separation prior to MS. We have previously described a separation method by capillary electrophoresis allowing the resolution of the three sulfated fucose isomers.[50] However this electrophoretic method could not be easily coupled to MS because it was carried out in non-aqueous electrolyte and in reversed polarity mode. This mode induces a reverse electro-osmotic flow, which is not compatible with a coupling to MS. Therefore we have investigated the electrophoretic separation of the fucose isomers in an aqueous electrolyte that ensured a forward electro-osmotic flow that is convenient for coupling. We first submitted 3-*O*-sulfated fucose to this CE-MS analysis in aqueous conditions. The fragmentation of the molecular ion at *m*/*z* 243 was carried out on-line and the total ion current (TIC) was recorded as well as the resulting signals corresponding to the different above-mentioned daughter ions. The total ion current was mainly due to daughter ion at *m*/*z* 97 (Fig. 4), confirming that the fragmentation of the 3-*O*-sulfated fucose leads only to sulfate loss. The electrophoregram obtained with the mixture of the three isomers exhibited a broad peak indicating a partial separation of the sulfated isomers in the aqueous electrolyte (Fig. 5). The corresponding TIC exhibited the same profile as the electrophoregram indicating that the partially resolved isomers eluted from the CE capillary were fully detected by MS (Fig. 5). At the beginning of the peak, the ion current was mainly due to daughter ion at *m*/*z* 97 in agreement with a previous study reporting that 3-*O*-sulfated fucose is the first isomer eluted from CE.[50] Then the signals corresponding to the daughter ions at *m*/*z* 139 and 183 arose accordingly to the elution of the two other isomers 2-*O*- and 4-*O*-sulfated. At the end of the electrophoresis peak, the signal at *m*/*z* 183 was particularly

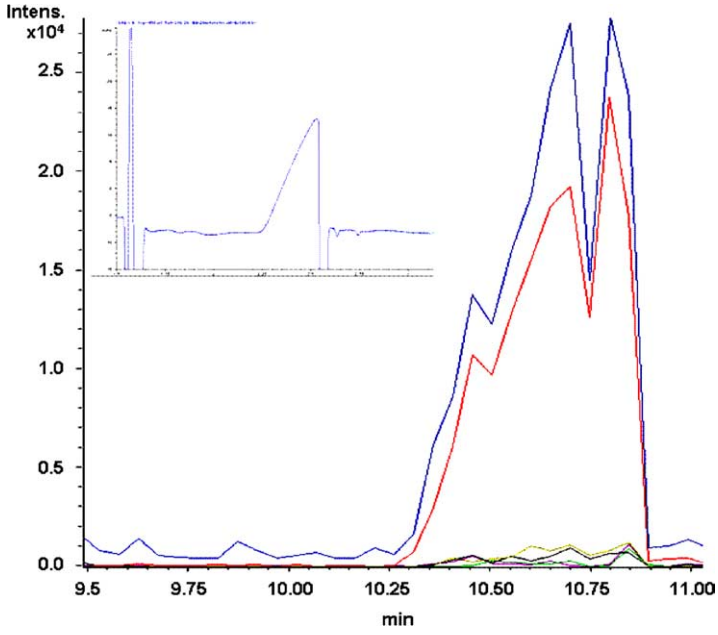

Figure 4. CE-ESIMS/MS analysis of the 3-*O*-sulfated fucose. The curves show the total ion current (TIC) upon fragmentation of the *m*/*z* 243 molecular ion (blue line), and the ion current of the resulting daughter ions at *m*/*z* 97 (red line), *m*/*z* 183 (dark green line), *m*/*z* 139 (purple line), and *m*/*z* 225 (dark line). Insert: Electropherogram of the 3-*O*-sulfated fucose (UV detection at 200 nm, capillary length 98 cm, details are given in the Experimental section).

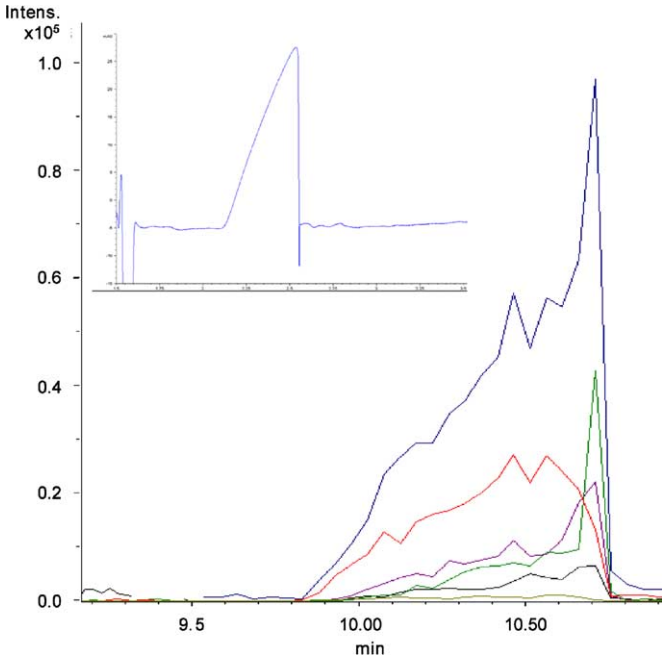

Figure 5. CE-ESIMS/MS analysis of the mixture of the three sulfated fucose isomers. The curves show the total ion current (TIC) upon fragmentation of the *m/z* 243 molecular ion (blue line), and the ion current of the resulting daughter ions at *m/z* 97 (red line), *m/z* 183 (dark green line), *m/z* 139 (purple line), and *m/z* 225 (dark line). Insert: Electropherogram of the mixture of the three isomers.

intense, consistent with the previously reported late elution of 4-*O*-sulfated fucose.[50]

When gathered, these data show clear differences between the three sulfated fucose isomers with regard to their fragmentation in ESIMS, in negative mode (Table 1). We used the nomenclature proposed by Domon and Costello[15] for the fragmentation of oligosaccharide (Chart 1).

According to this nomenclature, the daughter ions at *m/z* 183 and 139 were assigned to the fragment ions ^{0,2}A and ^{0,2}X, respectively, which originated from the internal cleavage of the fucopyranosyl ring. All the fragments detected contained the sulfate group. The ^{0,2}X ion at *m/z* 139 was formed from 2-*O*-sulfated fucose as expected. The ^{0,2}A ion was formed from 4-*O*-sulfated fucose as expected, but surprisingly it was not detected with 3-*O*-sulfated fucose. 4-*O*-Sulfated fucose also gave a very minor ^{0,3}A ion at *m/z* 153 whose counterpart for 3-*O*-sulfated fucose was the ^{0,3}X ion. Indeed, this ^{0,3}X ion was slightly detected at *m/z* 169 on the spectrum of the 3-*O*-sulfated isomer. In addition to these fragment ions, all three isomers exhibited loss of sulfate detected at *m/z* 97.

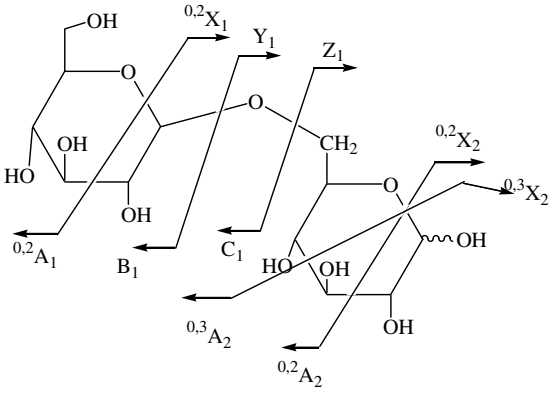

Chart 1. Nomenclature for glycosidic cleavage and cross-ring fragmentation according to Domon and Costello.[15]

Table 1. Ratios (*m/z*) of the fragment ions arising from cross-ring dissociations involving the C-1–O-5 bond cleavage (the ions experimentally observed are indicated in bold)

Sulfated fucose isomer	^{0,2}A	^{0,3}A	^{0,4}A	^{0,2}X	^{0,3}X	^{0,4}X
2-*O*-	103	73	43	**139**	169	199
3-*O*-	183	73	43	59	**169**	199
4-*O*-	**183**	**153**	43	59	89	199

Finally the two isomers 4-*O*-sulfated and 2-*O*-sulfated fucose could be differentiated based on their sulfated cross-ring fragments issued from the cleavage of the fucose ring, while the 3-*O*-sulfated isomer is characterized by the loss of sulfate group as the main fragmentation reaction. If we assume that the loss of sulfate is much more favored in the case of 3-*O*-sulfated fucose, the internal cleavage of this isomer should lead to neutral fragments that are not detected in the negative mode of ESIMS. Finally, it is worthy of note that all the fragment ions detected under MS/MS conditions incorporate the sulfate moiety.

3.3. Computational/mechanistic study

We carried out the molecular modeling of the conformation of the sulfated fucose isomers to get a better understanding of the reactivity of the three isomers upon ESIMS/MS conditions, and to determine the fragmentation mechanisms with respect to the position of the sulfate group. Given the very high number of possible isomers for sulfated L-fucose, we restricted our study to the most energetically favored pyranose $^1C_4$ chair conformation. For each sulfated fucose isomer (2-*O*-, 3-*O*-, and 4-*O*-), there is still a wide range of possible conformational arrangements taking into account the two α or β anomeric forms and the various possible orientations of the hydroxyl groups along the sugar ring that are driven by the formation of both O–H···O–H and O–H···O–S hydrogen bonds. We will discuss the calculated conformations in terms of hydrogen bonds and bond distances.

Sulfated fucose conformers are labeled **Cn-x**, **n** describing the sulfate position (2, 3, or 4) and **x** referring the conformer for a given sulfate position. This label is followed by (**α**) or (**β**) for α or β anomeric forms, respectively. The atomic labeling shown in Figure 1B is used throughout the text to describe the various sulfated fucose forms.

The geometries of the six most stable structures are given in Figures 6 and 7 for α and β anomers, respectively. Their corresponding absolute energy and relative energy are reported in Table 2. We can assume that these six optimized conformers do exist during our MS experiments since their relative energies are in the same range (4 kcal/mol) and are far below the collision energy typically used during MS/MS experiments (~25 kcal/mol). Moreover, the experimental collision energy is sufficient to allow the inter-conversion between conformers on the potential energy surface.[51]

We found that the conformations of lower energy systematically involve the α anomeric form, regardless of the sulfate position. The energetically most stable conformation was obtained for the 2-*O*-sulfated fucose conformer **C2-1**(**α**). For most of the hexoses, the α anomer has been traditionally thought to be more stable in the gas phase than the β form,[52] while the β anomer would be favored in water due to solvation effect. In fact, recent theoretical ab initio studies have shown that the α–β energy difference is so small either in the gas phase or in the aqueous phase that no conclusion can be drawn on the preference for the α/β anomeric form.[53–57] Accordingly, for each sulfated 2-*O*-, 3-*O*-, and 4-*O*-fucose isomer, we found that although the α anomer has always the lowest energy in the gas phase, there

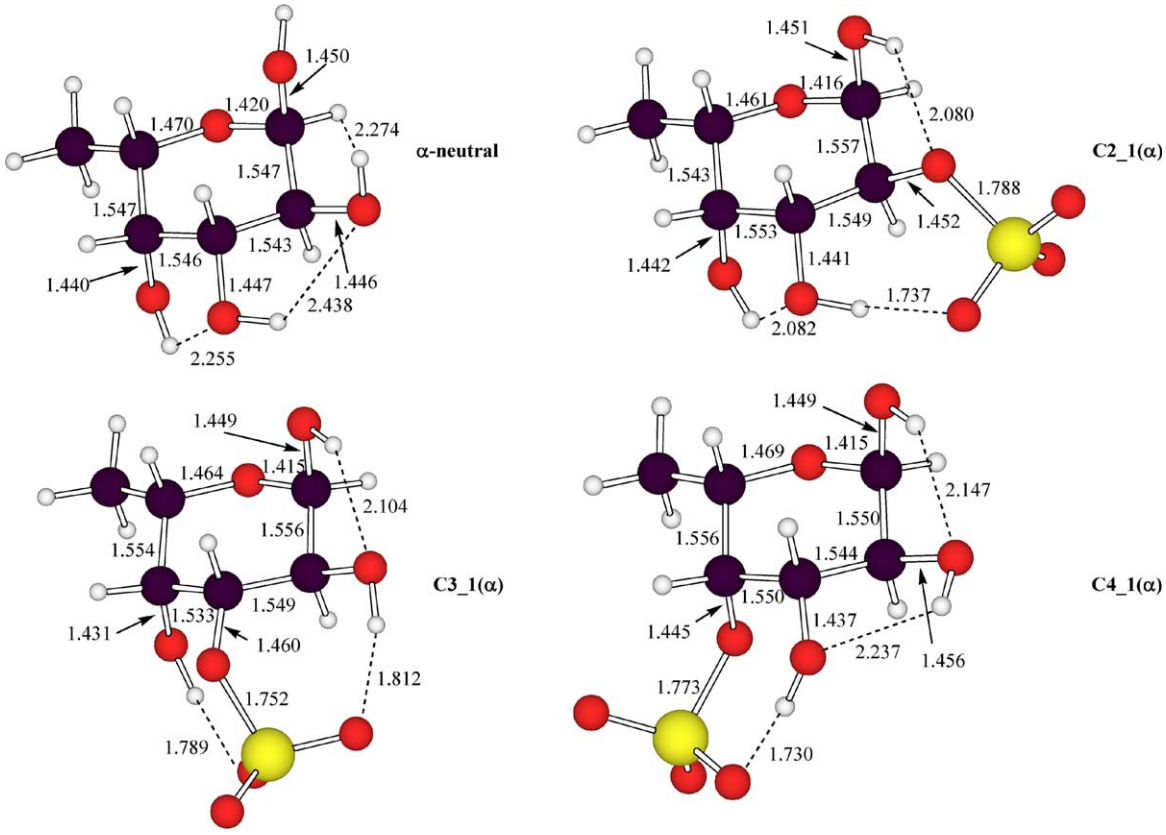

Figure 6. BLYP/6-31++G(d,p) geometries of the lowest energy structures of neutral and sulfated α-L-fucose (bond lengths are given in Angströms, hydrogen bonds are represented by dotted lines).

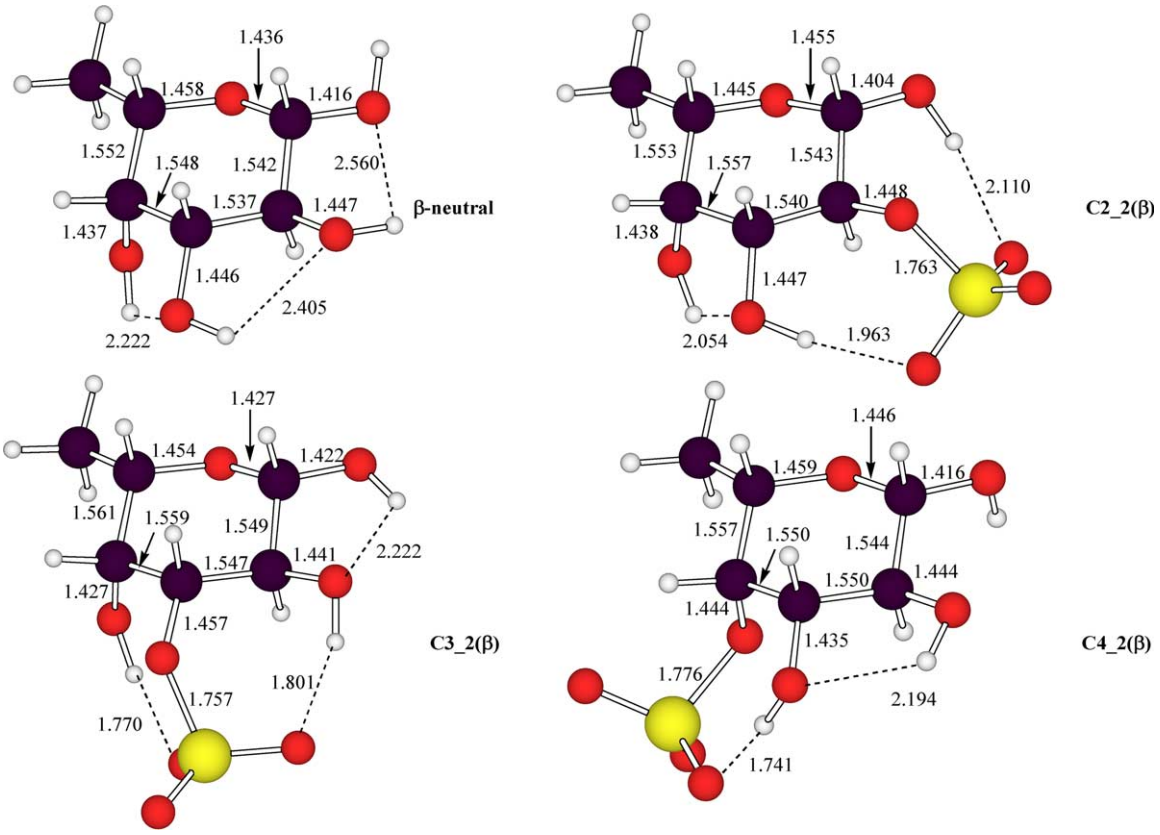

Figure 7. BLYP/6-31++G(d,p) geometries of the lowest energy structures of neutral and sulfated β-L-fucose (bond lengths are given in Angströms, hydrogen bonds are represented by dotted lines).

Table 2. Total (*E* in Hartree), zero-point vibrational energy (ZPVE in kcal/mol) and relative energies (Δ*E* in kcal/mol) of the six most stable structures of sulfated fucose obtained at the BLYP/6-31++G(d,p) level

Structure	*E*	ZPVE	Δ*E*[a]
C2-1(α)	−1235.0972932	117.7181	0.0
C2-2(β)	−1235.0954653	117.5985	1.1
C3-1(α)	−1235.0947365	117.8741	1.8
C3-2(β)	−1235.0909923	117.5867	3.9
C4-1(α)	−1235.0941815	117.6898	1.9
C4-2(β)	−1235.0913425	117.1750	3.3

[a] Include ZPVE correction.

is a very small energy difference between α and β geometries (1–2 kcal/mol).

Moreover, Molteni and Parrinello[55] have shown by ab initio molecular dynamics simulation that the α/β preference of glucose could be more related to the mobility behavior of the water molecules around the anomeric site rather than to energetical effects. It is also known that the anomeric composition of saccharides is affected by the presence of substituents.[58] In the case of sulfated fucose monomers, NMR experiments performed by Daniel et al.[38] in aqueous solution have revealed that the 3-*O*- and 4-*O*-sulfated fucose monomers adopt the β anomeric form, while the 2-*O*-sulfated fucose monomer is in the α anomeric form. Moreover, as mentioned above, the presence of the surrounding water solvent could change the α/β ratio, observed in the NMR experiments. We are currently investigating the behavior of water molecules around α/β sulfated fucoses by running ab initio molecular dynamics simulations in an aqueous environment.

Figures 6 and 7 reveal that all the structures exhibit several intramolecular hydrogen bonds. Our data show that the strongest hydrogen bonds are of O–H···O–S type (1.730–2.110 Å) formed between one S–O bond of the SO_3^- sulfate anion group and the neighboring O–H hydroxyl group. Our calculations highlight two particularly strong O–H···O–S hydrogen bonds only observed for the 3-*O*-sulfated fucose (**C3-1(α)** and **C3-2(β)** structures). These hydrogen bonds induce an important change in the pyranose ring: compared with neutral and 2-*O*- and 4-*O*-sulfated fucoses, we can see that the C-3–O-3 bond is lengthened while the O-3–S bond is reinforced. This feature is only encountered for the 3-*O*-sulfated isomer, and is consistent with the fact that the sulfate anion at *m*/*z* 97 (Fig. 3C) is the only fragment ion of high abundance observed on the MS/MS spectrum of this isomer.

Few data have been reported in the literature about the characterization of the positional isomers of sulfated hexoses.[59,60] Minamisawa and Hirabayashi[60] have shown using ESI/ITMS that both 3-*O*-sulfated glucose and 3-*O*-sulfated 2-acetamido-2-deoxy-D-glucose gives rise exclusively to the sulfate anion HSO_4^- (*m*/*z* 97). They proposed a fragmentation mechanism involving a nucleophilic substitution with the sulfate as the living group, and they made the assumption that this reaction occurs specifically when the sulfate group and the nucleophilic group (namely hydroxyl) are in a trans relationship. Our results support this assumption since the OH(2) group and the sulfate are indeed in trans relative orientation for the 3-*O*-sulfated isomer. A mechanism for this fragmentation is proposed in Chart 2b. However, other mechanisms for the formation of *m*/*z* 97 anion are very likely to occur because this ion is still observed in the MS/MS spectrum of 4-*O*-sulfated fucose for which a trans relative orientation is not possible. In addition, the sulfate anion is also observed on MS/MS spectra of peracetylated sulfated monosaccharides.[59]

Cross-ring cleavages are commonly observed on MS/MS spectra of deprotonated oligosaccharides. The ^{0,2}X and ^{0,2}A fragmentation patterns are the main cross-ring cleavages observed for the 2-*O*-sulfated fucose and the 4-*O*-sulfated fucose, respectively, during our CID experiments. These particular dissociations require both C-2–C-3 and C-1–O-5 bonds to be broken. One commonly accepted interpretation for these cleavages relies on the 'activation' of these bonds. The bond 'activation' may be viewed as the result of the elongation of the bonds in the sulfated fucose in comparison to ones in neutral fucose. This elongation leads to weakened bonds that are more likely to dissociate under MS/MS conditions. We thus compared the C-1–O-5 and C-2–C-3 bond lengths obtained for sulfated and neutral L-fucose structures (Figs. 6 and 7). It turns out that the most interesting information concerns the C-1–O-5 bond of β anomers. Indeed the **C2-2(β)** and **C4-2(β)** conformers display a strong increase (+0.010–0.020 Å) of the C-1–O-5 distance in going from the neutral to the sulfated fucose. With regard to the sulfated α conformers, they display a slight shortening of the C-1–O-5 distance when compared to the neutral form of fucose. Consequently, the 'activation' of the C-1–O-5 bond found for β 2-*O*- and 4-*O*-sulfated fucose isomers is consistent with the occurrence of ^{0,2}A and ^{0,2}X cross-ring cleavages for these two isomers. Additionally, in the particular case of the β 4-*O*-sulfated fucose monomer **C4-2(β)**, this activation is promoted by the significant elongation of C-2–C-3 (+0.013 Å). Taking into account that the pyranosidic ring of α anomers is not modified by sulfation, we may hypothesize that these forms would not undergo ^{0,2}A and ^{0,2}X cleavages upon collision, although these processes cannot be definitely ruled out.

The lack of cross-ring cleavage for the 3-*O*-sulfated fucose seems to indicate that the hydrogen of the hydroxyl group at C-3 plays an essential role in this

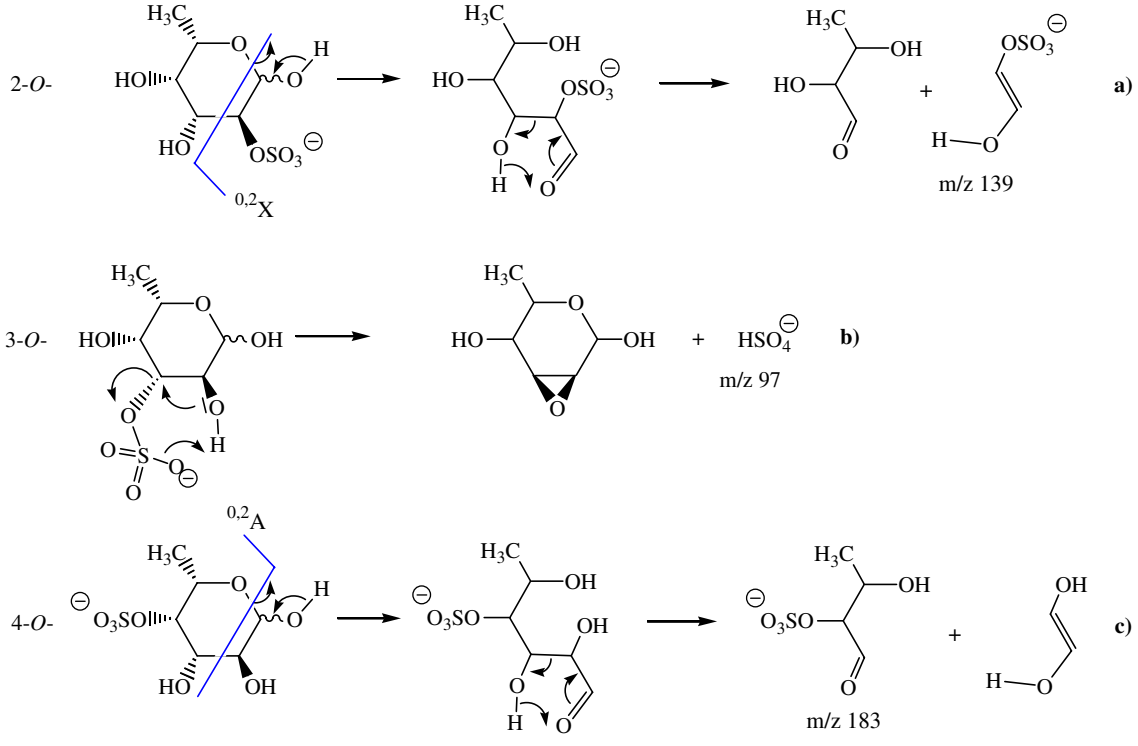

Chart 2.

fragmentation, as previously reported.[60,61] With respect to this observation and to the important activation of the C-1–O-5 bond, we propose a possible mechanism for these $^{0,2}X$ and $^{0,2}A$ cleavages (Chart 2a and c, respectively). It implies in the first step C-1–O-5 bond cleavage leading to an open keto form and then followed by a McLafferty rearrangement characterized by the scission of the C-2–C-3 bond. The mass to charge ratio of the ion generated (*m*/*z* 183 or 139) clearly depends on the initial position of the sulfate group and for the 2-*O*-sulfated isomer, this mechanism competes with the strong formation of HSO_4^- (*m*/*z* 97) because the sulfate group and the anomeric hydroxyl are in a trans orientation.

Finally, it is worth noting that both **C3-1(α)** and **C3-2(β)** conformers display a significant decrease of the C-1–O-5 distance (Figs. 6 and 7) in agreement with the lack of cross-ring cleavage for this isomer.

4. Conclusions

To our knowledge, this work is the first systematic study about the differentiation of the positional isomers of monosulfated fucose by mass spectrometry. The positional isomers regarding sulfation can be differentiated in MS/MS spectra through characteristic fragment ions. The loss of the hydrogenosulfate anion HSO_4^- is the main fragmentation reaction observed with the 3-*O*-sulfated fucose isomer. This feature has been also described for the sulfated monosaccharide 3-*O*-sulfated glucose[59,60] supporting the view of a fragmentation mechanism that involves a nucleophilic attack at the sulfate group by the adjacent transhydroxyl. The structure of the neutral fucopyranose ring has been previously reported,[62,63] and this study allowed us to provide for the first time the optimized structure for each sulfated fucose isomers by DFT calculations at a high optimized level. The conformational data reported here should be useful for the molecular modeling of fucoidan oligosaccharides,[64] and for a better understanding of the biological activities of fucoidan since the sulfation of fucose building blocks is likely to affect the conformational properties and bioreactivity of the polysaccharide.

Finally, negative electrospray ionization tandem mass spectrometry affords an efficient analytical method for the characterization of sulfated saccharides. Several recent reports demonstrated that the combination of ESIMS and MS/MS as used here allows the quantification of isomeric disaccharides present at different concentrations in a mixture.[65] Indeed each isomer exhibits a single fragmentation profile that is specific in terms of resulting daughter ions and in terms of relative intensities of each produced ion. The MS/MS sensitivity allows the detection and the quantification of an isomeric disaccharide present at level as low as 1%.[6] Used in conjunction with enzymatic depolymerization, ESIMS will be a powerful tool to analyze the complex structure of fucoidan and to probe for structural features, like the ratio between positional isomers, which could be viewed as chemotaxonomic marker.[66]

Acknowledgments

The authors thank Dr. Anne Imberty (CERMAV, Grenoble, France, http://www.cermav.cnrs.fr/glyco3d) for providing us a pdb structure file of neutral fucose, CINES (Montpellier, France) and IDRIS (Paris, France) for generous access to their computational facilities. M.P.G. and R.D. acknowledge Génopole-France for funding through an ATIGE 'Action Incitative de Génopole'.

References

1. Wormald, M. R.; Petrescu, A. J.; Pao, Y.-l.; Glithero, A.; Elliott, T.; Dwek, R. A. *Chem. Rev.* **2002**, *102*, 371–386.
2. Imberty, A.; Perez, S. *Chem. Rev.* **2000**, *100*, 4567–4588.
3. Laine, R. A. *Glycobiology* **1994**, *4*, 759–767.
4. Turnbull, J.; Powell, A.; Guimond, S. *Trends Cell Biol.* **2001**, *11*, 75–82.
5. Tumova, S.; Woods, A.; Couchman, J. R. *Int. J. Biochem. Cell Biol.* **2000**, *32*, 269–288.
6. Saad, O. M.; Leary, J. A. *Anal. Chem.* **2003**, *75*, 2985–2995.
7. Zaia, J.; Costello, C. E. *Anal. Chem.* **2001**, *73*, 233–239.
8. Zaia, J.; Costello, C. E. *Anal. Chem.* **2003**, *75*, 2445–2455.
9. Kuberan, B.; Lech, M.; Zhang, L.; Wu, Z. L.; Beeler, D. L.; Rosenberg, R. *J. Am. Chem. Soc.* **2002**, *124*, 8707–8718.
10. Henriksen, J.; Ringborg, L. H.; Roepstorrf, P. *J. Mass Spectrom.* **2004**, *39*, 1305–1312.
11. Thomsson, K. A.; Karlsson, H.; Hansson, G. C. *Anal. Chem.* **2000**, *72*, 4543–4549.
12. Thanawiroon, C.; Rice, K. G.; Toida, T.; Linhardt, R. J. *J. Biol. Chem.* **2004**, *279*, 2608–2615.
13. Zaia, J.; McClellan, J. E.; Costello, C. E. *Anal. Chem.* **2001**, *73*, 6030–6039.
14. Tadano-Aritomi, K.; Kubo, H.; Ireland, P.; Okuda, M.; Kasama, T.; Handa, S.; Ishizuka, I. *Carbohydr. Res.* **1995**, *273*, 41–52.
15. Domon, B.; Costello, C. E. *Glycoconjugate* **1988**, *5*, 397–409.
16. Percival, E. G. V.; McDowell, R. H. *Chemistry and Enzymology of Marine Algal Polysaccharides*; Academic Press: New York, 1967; pp 157–175.
17. Itoh, H.; Noda, H.; Amano, H.; Zhuang, C.; Mizuno, T.; Ito, H. *Anticancer Res.* **1993**, *13*, 2045–2052.
18. Pereira, M. S.; Mulloy, B.; Maurao, P. A. S. *J. Biol. Chem.* **1999**, *274*, 7656–7667.
19. Tissot, B.; Montdargent, B.; Chevolot, L.; Varenne, A.; Descroix, S.; Gareil, P.; Daniel, R. *Biochem. Biophys. Acta* **2003**, *1651*, 5–16.
20. Mourao, P. A. S.; Pereira, M. S. *Trends Cardiovascul. Med.* **1999**, *9*, 225–232.
21. Mourao, P. A. *Curr. Pharm. Des.* **2004**, *10*, 967–981.
22. Angstwurm, K. *Neurosci. Lett.* **1995**, *191*, 1–4.
23. Baba, M.; Schols, D.; Pauwels, R.; Nakashima, H.; De Clercq, E. *J. AIDS* **1990**, *3*, 493–499.

24. Mulloy, B.; Mourao, P. A.; Gray, E. *J. Biotechnol.* **2000**, *77*, 123–135.
25. Pereira, M. S.; Melo, F. R.; Mourao, P. A. *Glycobiology* **2002**, *12*, 573–580.
26. Pomin, V. H.; Pereira, M. S.; Valente, A. P.; Tollefsen, D. M.; Pavao, M. S.; Mourao, P. A. *Glycobiology* **2005**, *15*, 369–381.
27. Mulloy, B.; Ribeiro, A. C.; Alves, A. P.; Vieira, R. P.; Maurao, P. A. S. *J. Biol. Chem.* **1994**, *269*, 22113–22123.
28. Ribeiro, A. C.; Vieira, R. P.; Maurao, P. A. S.; Mulloy, B. *Carbohydr. Res.* **1994**, *225*, 225–240.
29. Patankar, M. S.; Oehninger, S.; Barnett, T.; Williams, R. L.; Clark, G. F. *J. Biol. Chem.* **1993**, *268*, 21770–21776.
30. Chevolot, L.; Mulloy, B.; Ratiskol, J.; Foucault, A.; Colliec-Jouault, S. *Carbohydr. Res.* **2001**, *330*, 529–535.
31. Chevolot, L.; Foucault, A.; Chaubet, F.; Kervarec, N.; Sinquin, C.; Fisher, A.-M.; Boisson-Vidal, C. *Carbohydr. Res.* **1999**, *319*, 154–165.
32. Ernst, S.; Langer, R.; Cooney, C. L.; Sasisekharan, R. *Crit. Rev. Biochem. Mol. Biol.* **1995**, *30*, 387–444.
33. Prime, S.; Dearnley, J.; Ventom, A. M.; Parekh, R. B.; Edge, C. J. *J. Chromatogr. A* **1996**, *720*, 263–274.
34. Turnbull, J. E.; Hopwood, J. J.; Gallagher, J. T. *Proc. Natl. Am. Soc.* **1999**, *96*, 2698–2703.
35. Merry, C. L. R.; Lyon, M.; Deakin, J. A.; Hopwood, J. J.; Gallagher, J. T. *J. Biol. Chem.* **1999**, *274*, 18455–18462.
36. Berteau, O.; McCort, I.; Goasdoue, N.; Tissot, B.; Daniel, R. *Glycobiology* **2002**, *12*, 273–282.
37. Daniel, R.; Berteau, O.; Jozefonvicz, J.; Goasdoue, N. *Carbohydr. Res.* **1999**, *322*, 291–297.
38. Daniel, R.; Berteau, O.; Chevolot, L.; Varenne, A.; Gareil, P.; Goasdoue, N. *Eur. J. Biochem.* **2001**, *268*, 5617–5626.
39. Frisch, M. J.; Trucks, G. W.; Schlegel, H. B.; Scuseria, G. E.; Robb, M. A.; Cheeseman, J. R.; Zakrzewski, V. G. Jr.; Montogomery, J. A.; Stratmann, R. E.; Burant, J. C.; Dapprich, S.; Millam, J. M.; Daniels, A. D.; Kudin, K. N.; Strain, M. C.; Farkas, O.; Tomasi, J.; Barone, V.; Cossi, M.; Cammi, R.; Mennucci, B.; Pomelli, C.; Adamo, C.; Clifford, S.; Ochterski, J.; Petersson, G. A.; Ayala, P. Y.; Cui, Q.; Morokuma, K.; Malick, D. K.; Rabuck, A. D.; Raghavachari, K.; Foresman, J. B.; Cioslowski, J.; Ortiz, J. V.; Baboul, A. G.; Stefanov, B. B.; Liu, G.; Liashenko, A.; Piskorz, P.; Komaromi, I.; Gomperts, R.; Martin, R. L.; Fox, D. J.; Keith, T.; Al-Laham, M. A.; Peng, C. Y.; Nanayakkara, A.; Gonzalez, C.; Challacombe, M.; Gill, P. M. W.; Johnson, B.; Chen, W.; Wong, M. W.; Andres, J. L.; Gonzalez, C.; Head-Gordon, M.; Replogle, E. S.; Pople, J. A. Gaussian, Pittsburgh PA, 1998.
40. Lee, C.; Yang, W.; Parr, R. *Phys. Rev. B* **1988**, *37*, 785–789.
41. Becke, A. D. *Phys. Rev. A* **1988**, *38*, 3098–3100.
42. Fonseca Guerra, C.; Bickelhaupt, F. M.; Snijders, J. G.; Baerends, E. J. *J. Am. Chem. Soc.* **2000**, *122*, 4117–4128.
43. Profeta, L. T. M.; Larkin, J. D.; Shaefer, H. F. *Mol. Phys.* **2003**, *101*, 3277–3284.
44. Gaigeot, M. P.; Sprik, M. *J. Phys. Chem. B* **2003**, *107*, 10344–10358.
45. Gaigeot, M. P.; Sprik, M. *J. Phys. Chem. B* **2004**, *108*, 7458–7467.
46. Chris, V.; Filip, S.; Miclaus, V.; Pinau, A.; Tanaselia, C.; Alamasan, V.; Vasilescu, M. *J. Mol. Struct.* **2005**, *744*, 363–368.
47. Piana, S.; Bucher, D.; Carloni, P.; Rothlisberger, U. *J. Phys. Chem. B* **2004**, *108*, 11139–11149.
48. Vargas, R.; Garza, J.; Hay, B. P.; Dixon, D. A. *J. Phys. Chem. A* **2002**, *106*, 3213–3218.
49. Morh, M.; Bryce, R. A.; Hillier, I. H. *J. Phys. Chem. A* **2001**, *105*, 8216–8222.
50. Descroix, S.; Varenne, A.; Goasdoue, N.; Abian, J.; Carrascal, M.; Daniel, R.; Gareil, P. *J. Chromatogr. A* **2003**, *987*, 467–476.
51. Csonka, G. I.; Elias, K.; Csizmadia, I. G. *J. Comput. Chem.* **1996**, *18*, 330–342.
52. Lemieux, R. U. *Explorations with Sugars: How Sweet It Was*; American Chemical Society: Washington, DC, 1990.
53. Cramer, C. J.; Truhlar, D. G. *J. Am. Chem. Soc.* **1993**, *115*, 5745–5753.
54. Jebber, K. A.; Zhang, K.; Cassady, C. J.; Chung-Philips, A. J. *J. Am. Chem. Soc.* **1996**, *118*, 10515–10524.
55. Molteni, C.; Parrinello, M. *J. Am. Chem. Soc.* **1998**, *120*, 2168–2171.
56. Polavarapu, P.; Edwig, C. S. *J. Comput. Chem.* **1992**, *13*, 1255–1261.
57. Salpin, J. Y.; Tortajada, J. *J. Mass Spectrom.* **2004**, *39*, 930–941.
58. Boons, G. J. Mono- and Oligosaccharides: Structures, Configuration and Conformation. In *Carbohydrate Chemistry*; Boons, G. J., Ed.; Thomson Science: London, 1998; pp 1–20.
59. Karlsson, N.; Karlsson, H.; Hansson, G. C. *J. Mass Spectrom.* **1996**, *31*, 560–572.
60. Minamisawa, T.; Hirabayashi, J. *Rapid Commun. Mass Spectrom.* **2005**, *19*, 1788–1796.
61. Carroll, J. A.; Willard, D.; Lebrilla, C. B. *Anal. Chim. Acta* **1995**, *307*, 431–447.
62. Lamba, D.; Segre, A. L.; Fabrizi, G.; Matsuhiro, B. *Carbohydr. Res.* **1993**, *243*, 217–224.
63. Rockey, W. M.; Dowd, M. K.; Reilly, P. J.; French, A. D. *Carbohydr. Res.* **2001**, *305*, 261–273.
64. Stortz, C. A. *Carbohydr. Res.* **2004**, *339*, 2381–2390.
65. Saad, O. M.; Ebel, H.; Uchimura, K.; Rosen, S. D.; Bertozzi, C. R.; Leary, J. A. *Glycobiology* **2005**, *15*, 818–826.
66. Bilan, M. I.; Grachev, A. A.; Ustuzhanina, N. E.; Shashkov, A. S.; Nifantiev, N. E.; Usov, A. I. *Carbohydr. Res.* **2004**, *339*, 511–517.